

1 **Title**

2 Toeholder: a Software for Automated Design and *In Silico* Validation of Toehold Riboswitches

3

4 **Authors and affiliations**

5

6 Angel F. Cisneros<sup>1,3,5,6†,\*</sup>, François D. Rouleau<sup>1,3,5,6†</sup>, Carla Bautista<sup>2,3,5,6‡</sup>, Pascale Lemieux<sup>1,3,5,6‡</sup>,

7 Nathan Dumont-Leblond<sup>4‡</sup>, on behalf of Team iGEM ULaval 2019

8

9 <sup>1</sup>Département de biochimie, microbiologie et bio-informatique, Université Laval, Quebec City, QC,  
10 Canada

11 <sup>2</sup>Département de biologie, Université Laval, Quebec City, QC, Canada

12 <sup>3</sup>Institut de biologie intégrative et des systèmes, Université Laval, Quebec City, QC, Canada

13 <sup>4</sup>Centre de recherche de l'Institut universitaire de cardiologie et de pneumologie de Québec,  
14 Quebec City, QC, Canada

15 <sup>5</sup>Centre de recherche en données massives de l'Université Laval, Université Laval, Quebec City,  
16 QC, Canada

17 <sup>6</sup>Regroupement québécois de recherche sur la fonction, l'ingénierie et la structure des protéines  
18 (PROTEO), Université Laval, Quebec City, QC, Canada

19

20 †These authors contributed equally to this publication

21 ‡These authors contributed equally to this publication

22

23 \*Corresponding authors:

24 Institut de biologie intégrative et des systèmes, Université Laval, Quebec City, QC, Canada, G1V  
25 0A6

26 E-mail address: [angel-fernando.cisneros-caballero.1@ulaval.ca](mailto:angel-fernando.cisneros-caballero.1@ulaval.ca)

27

28

29 **Keywords**

30

31 Toehold switch, Riboswitches, Molecular switch, Expression regulation

32 **Abstract**

33 Synthetic biology aims to engineer biological circuits, which often involve gene expression. A  
34 particularly promising group of regulatory elements are riboswitches because of their versatility  
35 with respect to their targets, but early synthetic designs were not as attractive because of a  
36 reduced dynamic range with respect to protein regulators. Only recently, the creation of toehold  
37 switches helped overcome this obstacle by also providing an unprecedented degree of  
38 orthogonality. However, a lack of automated design and optimization tools prevents the  
39 widespread and effective use of toehold switches in high throughput experiments. To address  
40 this, we developed Toeholder, a comprehensive open-source software for toehold design and *in*  
41 *silico* comparison. Toeholder takes into consideration sequence constraints from experimentally  
42 tested switches, as well as data derived from molecular dynamics simulations of a toehold switch.  
43 We describe the software and its *in silico* validation results, as well as its potential applications  
44 and impacts on the management and design of toehold switches.

## 45 **1.Introduction**

### 46 *1.1 Riboswitches*

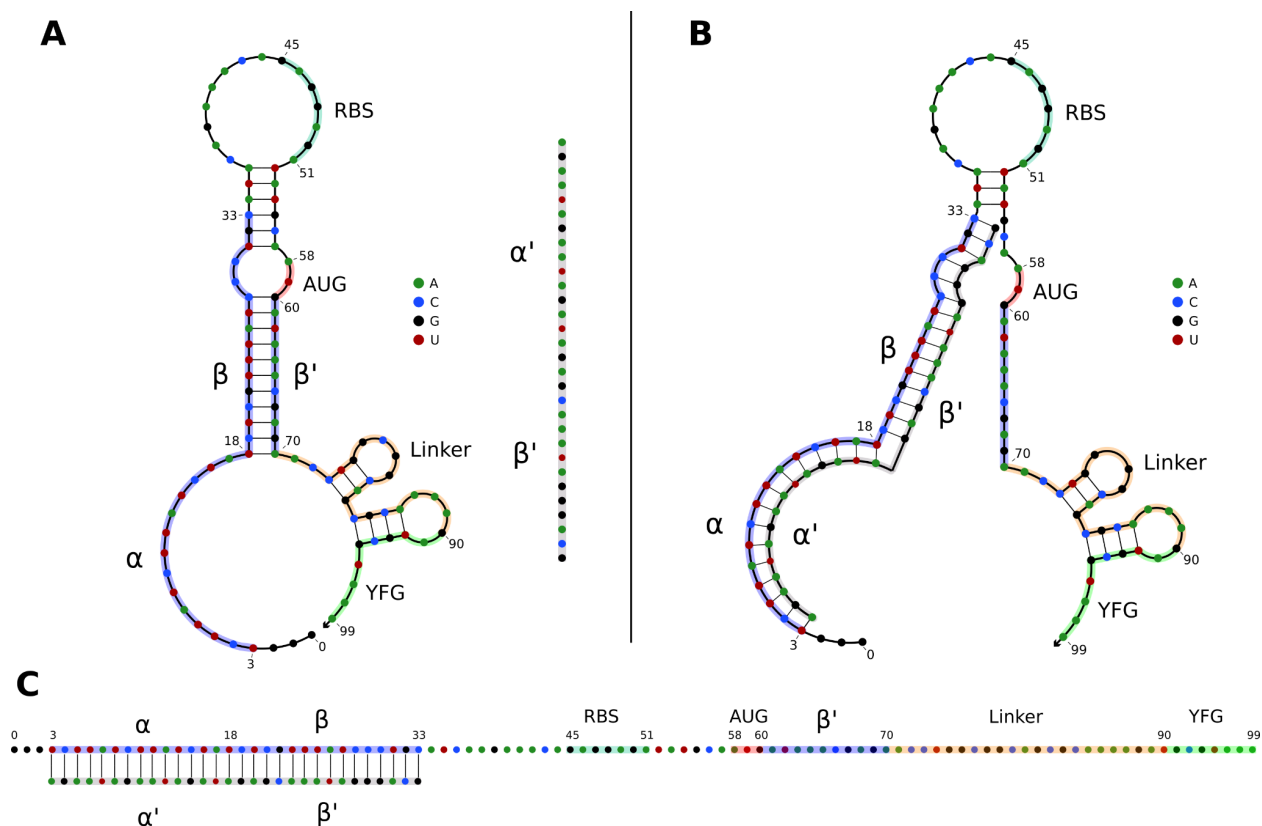
47

48 All biological systems, be they naturally occurring or synthetic, rely on finely tuned interactions of  
49 their components. The precise regulation of these interactions is often critical to proper system  
50 functions, and there exist, in nature, many such regulatory mechanisms. A particularly interesting  
51 group of regulatory elements are riboswitches - RNA molecules, which typically predominate  
52 within the 5'-untranslated region (UTR) of prokaryotic protein coding transcripts and that fold into  
53 specific secondary and tertiary structures capable of regulating transcription and translation,  
54 thereby optimizing the use of resources (Findeiß et al. 2017). Riboswitches have been observed  
55 in bacteria (Winkler, Nahvi, and Breaker 2002), archaea (Gupta and Swati 2019), and in some  
56 fungi and plants (Sudarsan, Barrick, and Breaker 2003). They respond to a wide range of stimuli,  
57 for instance metabolite concentrations, and their prevalence and versatility in nature makes them  
58 attractive for the design of synthetic biological circuits (Mandal and Breaker 2004; Garst, Edwards,  
59 and Batey 2011).

60

61 Efforts to leverage the potential of riboswitches for synthetic biology have led to several different  
62 designs. Out of these, toehold switches have recently been put in the spotlight as a versatile tool  
63 with an unprecedented dynamic range and orthogonality (orthogonality meaning that the system  
64 is self-contained and has as little spurious effects as possible on other cellular functions) (Green  
65 et al. 2014). Toehold switches are single-stranded RNA molecules containing the necessary  
66 elements for the translation of a reporter protein: its coding sequence, a ribosome binding site,  
67 and a start codon. They fold into a specific hairpin-like secondary structure that blocks the  
68 ribosome's access to its binding site and the first start codon on the RNA strand, therefore  
69 preventing translation of the coded protein further downstream (OFF state). The hairpin is  
70 designed such that when the toehold riboswitch is in the presence of its DNA or RNA "trigger"  
71 sequence, the hairpin unfolds (ON state), hence giving access to the ribosome binding site and  
72 the start codon to enable translation (Green et al. 2014) (Figure 1). As a result, the reporter protein  
73 can be used to confirm the presence of the trigger sequence in a sample, which opens a wide  
74 variety of potential applications for biosensors.

75



76  
77

78 **Figure 1: A)** OFF state of a typical toehold switch. Nucleotides (nt) 3 to 33 ( $\alpha$ ,  $\beta$ ) are  
79 complementary to the trigger sequence ( $\alpha'$ ,  $\beta'$ ), nt 45 to 51 are the RBS, nt 58 to 60 are the  
80 upstream start codon, nt 70 to 90 are the linker sequence, nt 90 and downstream are part of the  
81 regulated gene of interest. The trigger sequence ( $\alpha'$ ,  $\beta'$ ) is shown in grey for reference next to the  
82 toehold switch. **B)** Intermediate state of a toehold switch when it first binds to its trigger sequence.  
83 **C)** ON state of typical toehold switch, where it is stably bound to its trigger sequence, and  
84 translation can occur.

85  
86  
87

## 1.2 Applications

88 Despite being a fairly recent technology, toehold switches have already been applied to various  
89 fields. Applications include orthogonal systems to regulate gene expression *in vivo* (Green et al.  
90 2014), diagnostic tools for RNA virus detection (ebola (Magro et al. 2017), coronavirus (Park and  
91 Lee 2021), norovirus (Ma et al. 2018)), organ allograft rejection detection (Chau and Lee 2020),  
92 and even logic gates for gene regulation in synthetic systems (Green et al. 2014, 2017) for  
93 pharmaceutical and medical purposes, for example as targets for novel antibiotics (Blount and  
94 Breaker 2006) or in gene therapy (Nshogozabahizi et al. 2019). Toehold switch-based technology  
95 is highly modifiable and cost-effective, making it a very interesting tool to address present and  
96 future challenges, and holds great promise in being extendable to numerous and varied purposes.

97  
98  
99

## 1.3 Design

100 When the toehold switch is properly designed, the hairpin will natively fold on itself as the RNA is  
101 transcribed, following Watson-Crick canonical hydrogen bonds-based pairing. In absence of the  
102 trigger sequence, it will be most stable when in its OFF (hairpin/unbound) conformation, therefore  
103 preventing spurious activation and translation of the downstream open reading frame (ORF). In  
104 presence of the trigger sequence, the higher Watson-Crick homology between the switch/trigger  
105 structure than within the switch itself will favor the unfolding of the hairpin (the ON state), allowing  
106 for downstream translation.

107

108 However, the design of toehold switches is not always straightforward. As proper repression of  
109 the downstream ORF relies on the secondary structure to avoid leakage and spurious translation,  
110 the sequence of the hairpin structure, and therefore the sequence of the trigger, is critical.  
111 Depending on the trigger sequence, many of the regulatory parts of the toehold switch, including  
112 the RBS and first start codon, and to a lesser extent, the linker sequence, can interfere with proper  
113 folding of the hairpin (Findeiß et al. 2017). There are therefore important sequence constraints to  
114 observe when designing good quality toehold switches, in which signal leakage (OFF activity) is  
115 minimized, while maximizing protein expression (ON activity) when bound to its trigger. Therefore,  
116 studying the molecular dynamics of toehold riboswitches could help identify ways to improve their  
117 design.

118

119 Over the past few years, leaps and bounds have been made in the field of toehold switch design.  
120 Vast improvements have been made on their ON/OFF ratios/fold increase, dynamic expression  
121 levels, and signal leakage, and some sites on the trigger sequence have been identified as being  
122 key to hairpin folding, but a standardised “best-practice” when designing toeholds is still lacking.  
123 Since few high-throughput datasets on experimentally tested toeholds are available,  
124 understanding what makes some better than others remains difficult (Green et al. 2014). As of  
125 right now, the main limiting factor in the broader applications of toehold technology is the  
126 exploratory aspect of designing toehold switches, as well as intrinsic limitations imposed by  
127 essential switch elements (Ausländer and Fussenegger 2014).

128

129 In 2019, our iGEM team designed a project around the real-life applications of toehold switches.  
130 Thus, we looked for available tools that could aid the design of these riboswitches. To the best of  
131 our knowledge, the only available tools for the design of toehold riboswitches were the NUPACK  
132 design suite (Zadeh et al. 2011) and a tool designed by Team iGEM CUHK 2017 (To et al. 2018).  
133 However, these tools have a high entry level difficulty, especially when setting up a methodology  
134 and when analyzing the results. To address this, our 2019 iGEM team decided to design an open-  
135 source software to make working with toehold switches more accessible, and hopefully allow for  
136 broader applications of toehold-based technologies. We created Toeholder, a comprehensive  
137 software for toehold design and *in silico* comparison. Toeholder takes into consideration  
138 sequence constraints described by Green et al (2014), as well as data derived from our molecular  
139 dynamics simulations of a toehold switch. In the present work, we describe the software and its  
140 *in silico* validation results, as well as its potential applications and impact on the management and  
141 design of toeholds.

142

143

## 144 **2. Materials and methods**

### 145 *2.1 Molecular dynamics simulations of a toehold switch*

146  
147 Molecular dynamics simulations were performed on a toehold switch from Green et al. (2014) to  
148 study the dynamics of its predicted secondary and tertiary structure. We hypothesised that  
149 fluctuations in the formation of hydrogen bonds in the hairpin of the toehold switch could lead to  
150 spontaneous unwinding of the hairpin, causing the residual OFF signal observed in experiments.  
151 As such, we reasoned that studying the dynamics of the structure might provide a broader  
152 understanding of the stability of the base pairing in toehold switches.

153  
154 Sequences from previously designed toehold switches were downloaded from Green et al.  
155 (2014). Toehold switch number 1 from table S3 was selected for further modeling because it  
156 provided the highest ON/OFF ratio. Its sequence was used to generate a secondary structure  
157 with NUPACK (Zadeh et al. 2011) with the rna1995 parameters (Serra and Turner 1995; Zuker  
158 2003; Dirks and Pierce 2003) and a temperature of 37°C. Later, the sequence and the predicted  
159 secondary structure were submitted to the RNAComposer online server (Popenda et al. 2012;  
160 Purzycka et al. 2015) to obtain a 3D model. The quality of the 3D model was validated with  
161 MOLProbity (V. B. Chen et al. 2010) (Table S1). The 3D structure of the toehold switch was  
162 introduced in a square water box (146 Å x 146 Å x 146 Å) using the online CHARMM-GUI server  
163 (Jo et al. 2008; Lee et al. 2016) with a salt concentration of 0.15 M NaCl. Energy minimization  
164 was performed using an NPT equilibration at a constant temperature of 298.15 K. Molecular  
165 dynamics simulations were run with the NAMD simulation engine (Phillips et al. 2005) with explicit  
166 solvent and periodic boundary conditions for a total length of 40 ns using the CHARMM36 force  
167 field and the TIP3P water model.

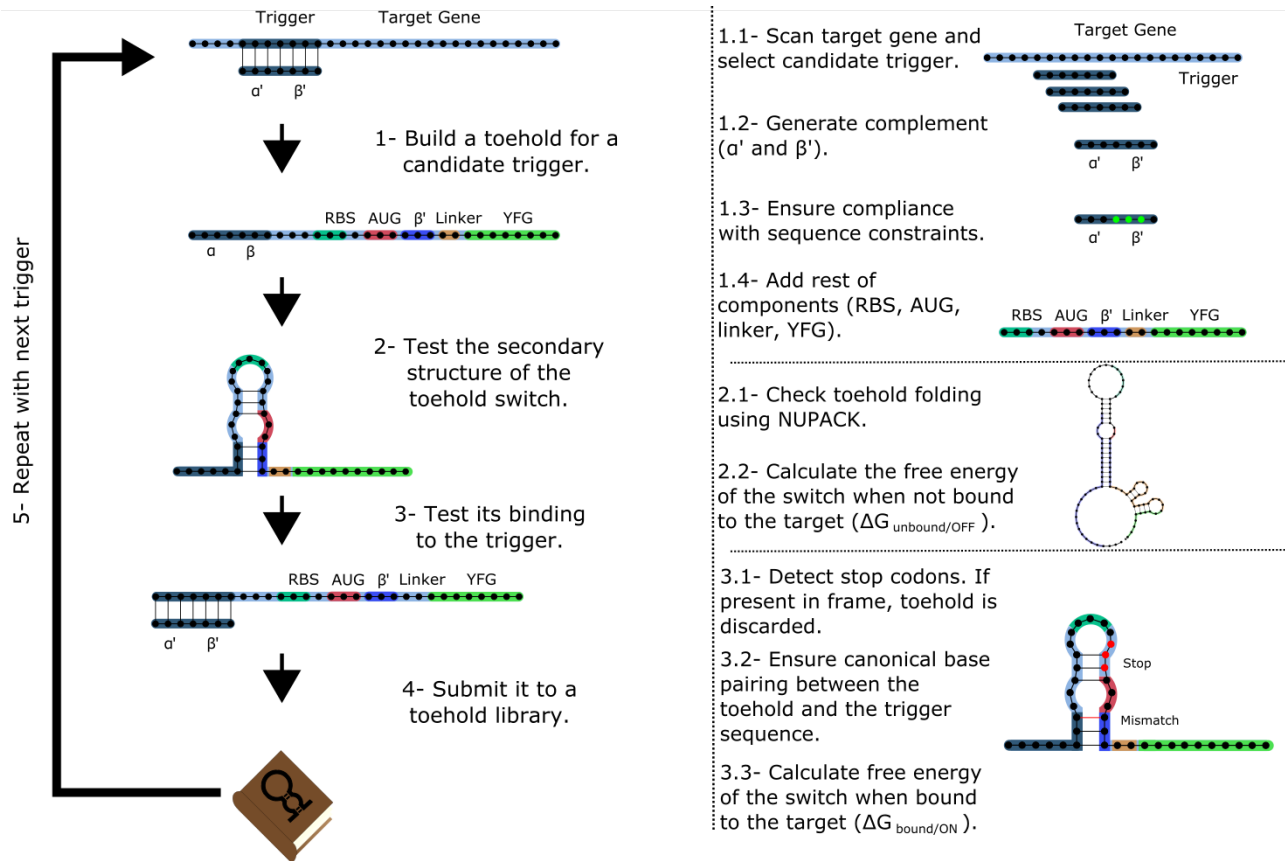
168  
169 Molecular dynamics simulations (Supplementary video 1) were analyzed using VMD (Humphrey,  
170 Dalke, and Schulten 1996). The stability of the hairpin of the toehold riboswitch was evaluated by  
171 measuring the persistence of hydrogen bonds throughout the simulation. The percentage of  
172 frames in the simulation in which a hydrogen bond is detected (occupancy) was measured using  
173 VMD with a distance cut-off of 3 Å and an angle cut-off of 20°. Hydrogen bonds were classified  
174 as either canonical (if they appear in the desired secondary structure) or non-canonical (if they do  
175 not).

### 176 177 *2.2 Designing toehold switches with Toeholder*

178  
179 In parallel to the previous tests, an automated workflow to design and test toehold switches was  
180 created to accelerate those processes. The Toeholder software is publicly available on GitHub at  
181 <https://github.com/igem-ulaval/toeholder>. As of publication, it is the first iteration of the program  
182 built on the observations of Green et al. (2014). Improvements based on our molecular dynamics  
183 simulations remain to be made.

184  
185 The Toeholder workflow for designing toehold switches is shown in Figure 2. Briefly, Toeholder  
186 receives a target gene and other parameters (length of trigger region bound to target, length of  
187 trigger in hairpin, reporter gene sequence) as input that will be used to perform a sliding window

188 scan of the target sequence. The sliding window is used to determine the trigger sequence, that  
 189 is, the complement of the intended target sequence. Afterwards, the sequence that will close the  
 190 hairpin is added as the complement of the second part of the trigger sequence. The loop and  
 191 linker regions are taken from the sequence of toehold 1 from table S3 from Green et al. (2014).  
 192 Once the candidate toehold for that window has been produced, the sliding window advances by  
 193 one nucleotide. Toeholder produces potential switches for candidates along the entire length of  
 194 the target gene.  
 195



196  
 197 **Figure 2. Workflow used by Toeholder to design toehold riboswitches.** From a target gene,  
 198 a sliding window is used to determine candidate triggers and its complementary sequence is used  
 199 to produce the hairpin. The rest of the elements of the toehold riboswitch are then added to the  
 200 sequence. The secondary structure, binding energy, and binding accuracy of the toehold  
 201 riboswitch are then tested *in silico*. Toeholder saves the results and moves the sliding window by  
 202 one nucleotide to work with the following candidate trigger.  
 203

204 Toehold switches produced by Toeholder are then tested automatically using NUPACK (Zadeh  
 205 et al. 2011). The minimum free energy secondary structures of the proposed toehold switch and  
 206 the target mRNA are generated separately, as well as the minimum free energy secondary  
 207 structure for the proposed toehold switch bound to the target mRNA. The calculated free energies  
 208 from these three tests are used to determine the changes in free energy ( $\Delta\Delta G$ ) (Formula 1).  
 209

$$\Delta\Delta G_{binding} = \Delta G_{bound/ON} - (\Delta G_{unbound/OFF} + \Delta G_{target}) \quad (1)$$

210

211 The potential switches with the lowest  $\Delta\Delta G_{binding}$  are considered the most likely to offer good  
212 performance. Furthermore, the predicted structure of the toehold switch bound to the target  
213 mRNA is used to test if the hybridized region is the intended target. Toehold switches that bind  
214 perfectly to the intended target are prioritized over those that are predicted to bind partially. The  
215 final tests involve looking for stop codons in the region of the toehold switch that would be used  
216 for translation, which results in a toehold switch being discarded, as well as ensuring canonical  
217 base pairing along the hairpin structure. Finally, only switches which respect suggested forward  
218 engineered sequence constraints based on experimental evidence from Green et al. (2014) (2  
219 G:C / 1 A:U base pairing at the bottom of the hairpin, 3 A:U base pairing at the top of the hairpin)  
220 are passed to the output.

221

### 222 2.3 Validation of Toeholder

223

224 Toeholder was created as part of a bigger project, A.D.N. (Air Detector of Nucleic Acids), that was  
225 meant to detect pathogenic viruses in the air through a combination of toeholds based biosensors  
226 and microfluidics. Therefore, the Toeholder workflow (see section 2.2) was used to design and  
227 test *in silico* toehold switches for seven different targets. These targets were selected on the basis  
228 of feasibility of our iGEM team working with them in a laboratory (*oxyR* from *Escherichia coli*, two  
229 CDS from the Phi6 bacteriophage, an ORF from the bacteriophage PR772) or viruses that can  
230 represent health concerns (norovirus, measles virus H1, human alphaherpesvirus 3). The *in silico*  
231 characterization of the switches and their production process gave us a substantial validation of  
232 the initial workflow. The resulting switches, as well as the accession numbers of the target  
233 sequences are detailed in Table S2. Ultimately, the three switches with the lowest  $\Delta\Delta G_{binding}$  and  
234 perfect matches to their respective triggers for each target were selected and submitted as parts  
235 to the iGEM registry. Selecting three candidates per target allows for a greater probability of  
236 identifying a successful switch, since our iGEM team was unable to validate them experimentally.

237

238

239 Toeholds were also aligned to several reference genomes to test their predicted specificity and  
240 versatility using blastn for short sequences (Camacho et al. 2009). These reference genomes  
241 were selected based on the possibility of being present in the same samples as the target in a  
242 real application (*Escherichia coli*, *Homo sapiens*, MS2 phage, PM2 phage, Norovirus,  
243 Herpesvirus) and to determine if the trigger sequence of a toehold switch was present in several  
244 different measles virus strains (B3, C2, D4, D8, G2, H1).

245

246

247

## 248 3.Results

### 249 3.1 Analysis of molecular dynamics simulations

250



251 The modeled structure of the toehold riboswitch from Green et al. (Green et al. 2014) remained  
252 stable throughout the molecular dynamics simulation (supp. video 1). In particular, the hairpin of  
253 the toehold riboswitch did not unwind, which would have led to the unwanted expression of the  
254 reporter gene. The most flexible regions of the structure were the two ends of the molecule, as  
255 expected, because base pairing in these regions is very limited.

256

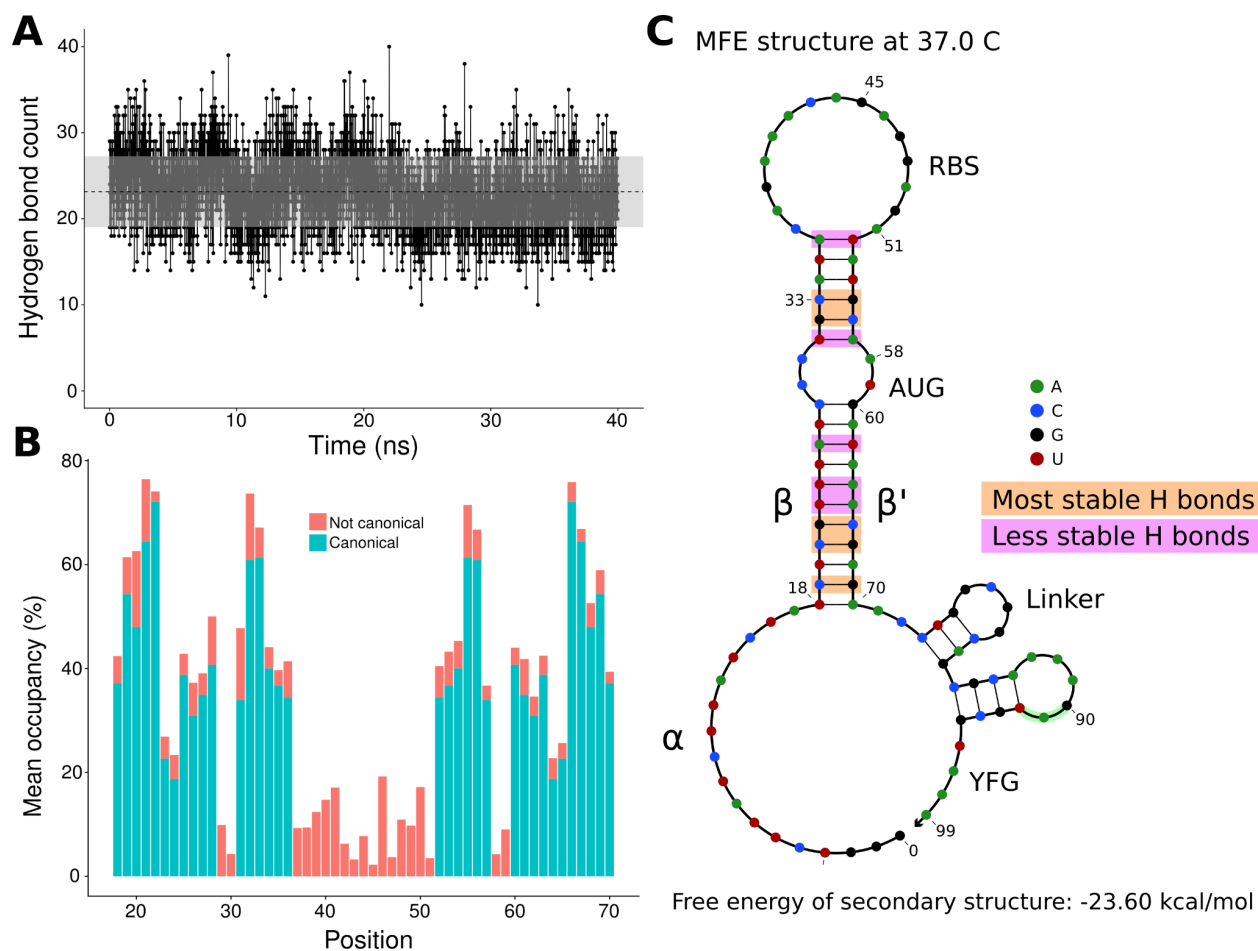
257 Since the hairpin relies primarily on hydrogen bonds resulting from base pairing, we did a  
258 quantitative analysis on hydrogen bonds throughout the molecular dynamics simulation. We found  
259 that the number of hydrogen bonds remains relatively stable throughout the simulation (Figure  
260 3A), which is consistent with our observation of the hairpin not unwinding. We then set out to  
261 identify the positions in the hairpin that were responsible for the fluctuations observed in the  
262 number of hydrogen bonds. We measured the occupancy, i.e. the percentage of frames of the  
263 simulation in which the hydrogen bond is observed, of each intended hydrogen bond in the hairpin  
264 (Figure 3B). Since base pairing includes multiple hydrogen bonds (two for each A:U pair and three  
265 for each G:C pair), each position is represented by the mean of the occupancies of its hydrogen  
266 bonds. By comparing the occupancies at each position, we identified the five most stable  
267 (hydrogen bonds between nucleotides 19, 21, 22, 32, and 33 and their complements) and the  
268 five least stable hydrogen bonds (nucleotides at positions 23, 24, 26, 31, and 36 with their  
269 complements) of the hairpin of the simulated toehold switch (Figure 3C). Thus, we hypothesized  
270 that GC content at these positions of interest could facilitate hairpin unwinding and contribute to  
271 the high ON/OFF ratio of toehold switch 1.

272

273

274

275

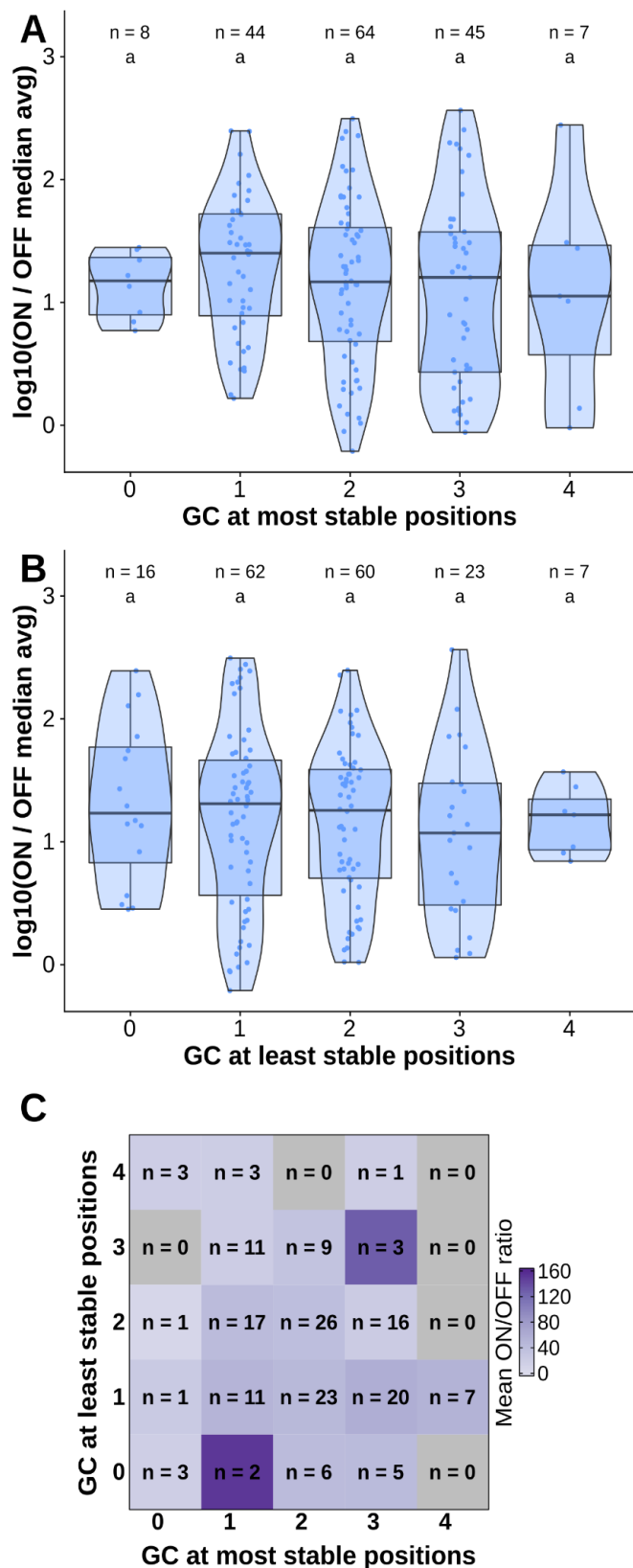


276  
277

**Figure 3. Analysis of hydrogen bonds throughout the molecular dynamics simulation. A)** Number of hydrogen bonds observed at every time point of the simulation. The black dashed line indicates the mean number of hydrogen bonds, and the shaded region indicates one standard deviation above and under the mean. **B)** Average occupancy of canonical (as determined by the predicted secondary structure) and not canonical hydrogen bonds throughout the molecular dynamics simulation at each position. **C)** Secondary structure diagram showing the positions with the most and least stable hydrogen bonds in the hairpin.

To test the contribution of GC content at these positions of interest to ON/OFF ratio, we reanalyzed the available dataset of 168 first-generation toehold switches from Green et al. (2014). We labeled each of the toehold switches based on the number of positions of interest from the molecular dynamics simulation containing GC, except for position 36 since design constraints require A:U pairing at that position. However, our statistical test (ANOVA with Tukey's test for honest significant differences) showed that any differences in ON/OFF ratio for toehold switches with GC at the most stable positions (Fig. 4A) or at the least stable positions (Fig. 4B) were not statistically significant. To complement the analysis, we analyzed the distribution ON/OFF ratio based on the combination of GC content at both the most stable and least stable positions but observed that the available dataset underrepresents most of the possible combinations, with no switches sharing the pattern observed in toehold switch 1 of GC at all of the most stable positions

297 and AU at all of the least stable positions (Fig. 4C). Thus, our results suggest that neither the  
298 most stable nor the least stable positions could explain the ON/OFF ratio on their own, but we  
299 cannot fully confirm the relevance of these positions based on currently available experimental  
300 data.



301

302

303

**Figure 4. Contributions of GC content at positions of interest from the molecular dynamics simulation.** Data from first-generation toehold riboswitches from Green et al. 2014 were used.

304 **A)** ON/OFF ratio for toehold riboswitches based on GC at the most stable positions for the  
305 molecular dynamics simulation of the best forward engineered toehold from Green et al. 2014. **B)**  
306 ON/OFF ratio based on GC at the least stable positions from the molecular dynamics simulation.  
307 **C)** Combinations of GC at the most stable and least stable positions and the mean ON/OFF ratio  
308 for each combination. Numbers of toehold riboswitches in each group are indicated.  
309

### 310 *3.2 Validating toehold riboswitches designed by Toeholder*

311

312 All toehold riboswitches designed by Toeholder were tested *in silico* to evaluate their quality. Here,  
313 we show how riboswitches designed with Toeholder for seven different targets scored in our tests.  
314

315 The first test validates the secondary structure of the riboswitch using NUPACK (Zadeh et al.  
316 2011). Our riboswitches tended to have a similar secondary structure to the one with the highest  
317 ON/OFF ratio designed by Zadeh et al. (2011). The average secondary structures for riboswitches  
318 generated for each of the seven different targets and the riboswitch from Zadeh et al. (2011) as  
319 the reference are shown in table S2. Average secondary structures were generated by taking the  
320 most frequent state for each position in the set of sequences for the same target. Importantly, the  
321 main hairpin and the smaller one closer to the reporter gene are preserved in these average  
322 secondary structures, indicating that toehold riboswitches designed by Toeholder fold into a  
323 desirable secondary structure.  
324

325 The following tests evaluate the predicted binding of the toehold riboswitches to the target. The  
326 distributions of  $\Delta\Delta G_{\text{binding}}$  values for every toehold riboswitch candidate produced for the seven  
327 targets are shown in Figure 5A. Since all the  $\Delta\Delta G_{\text{binding}}$  are negative, the bound state is more  
328 stable for all of our riboswitches than the unbound state.  
329

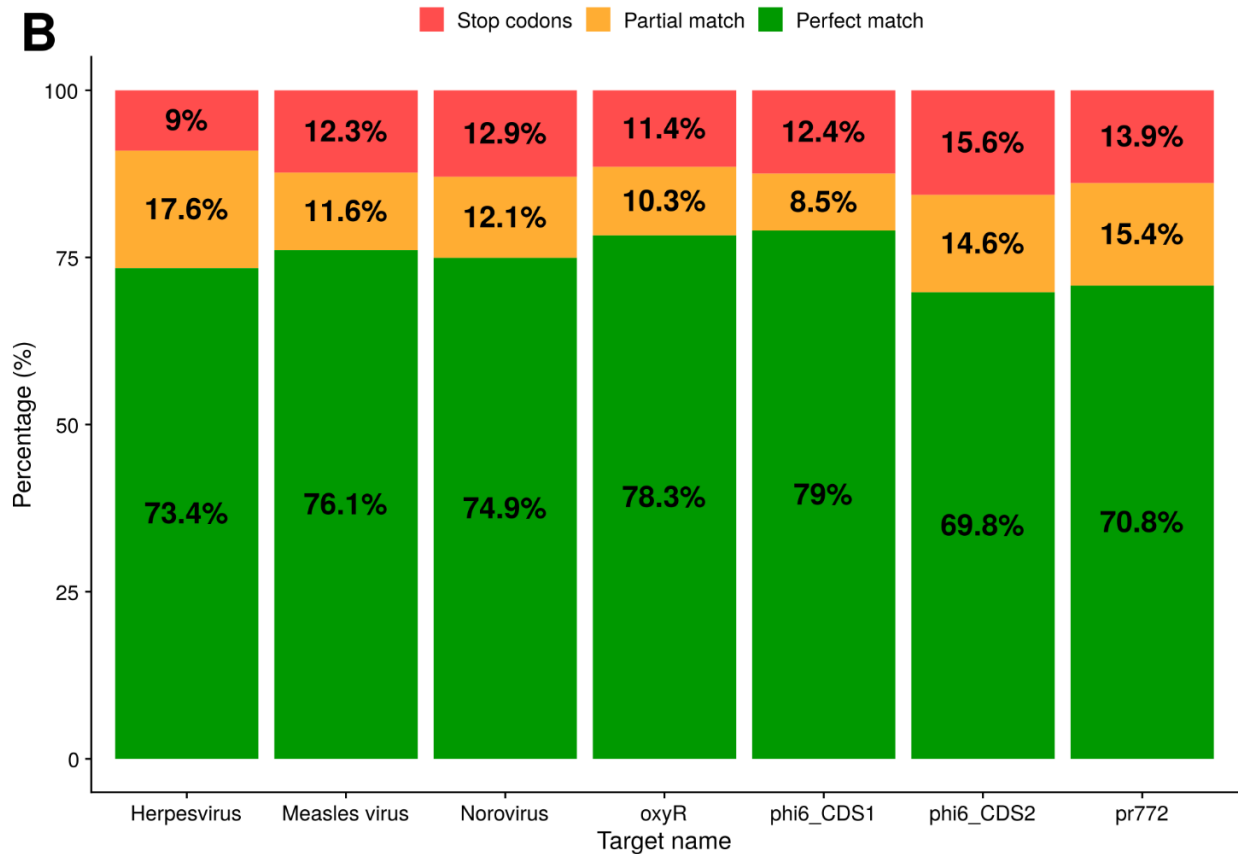
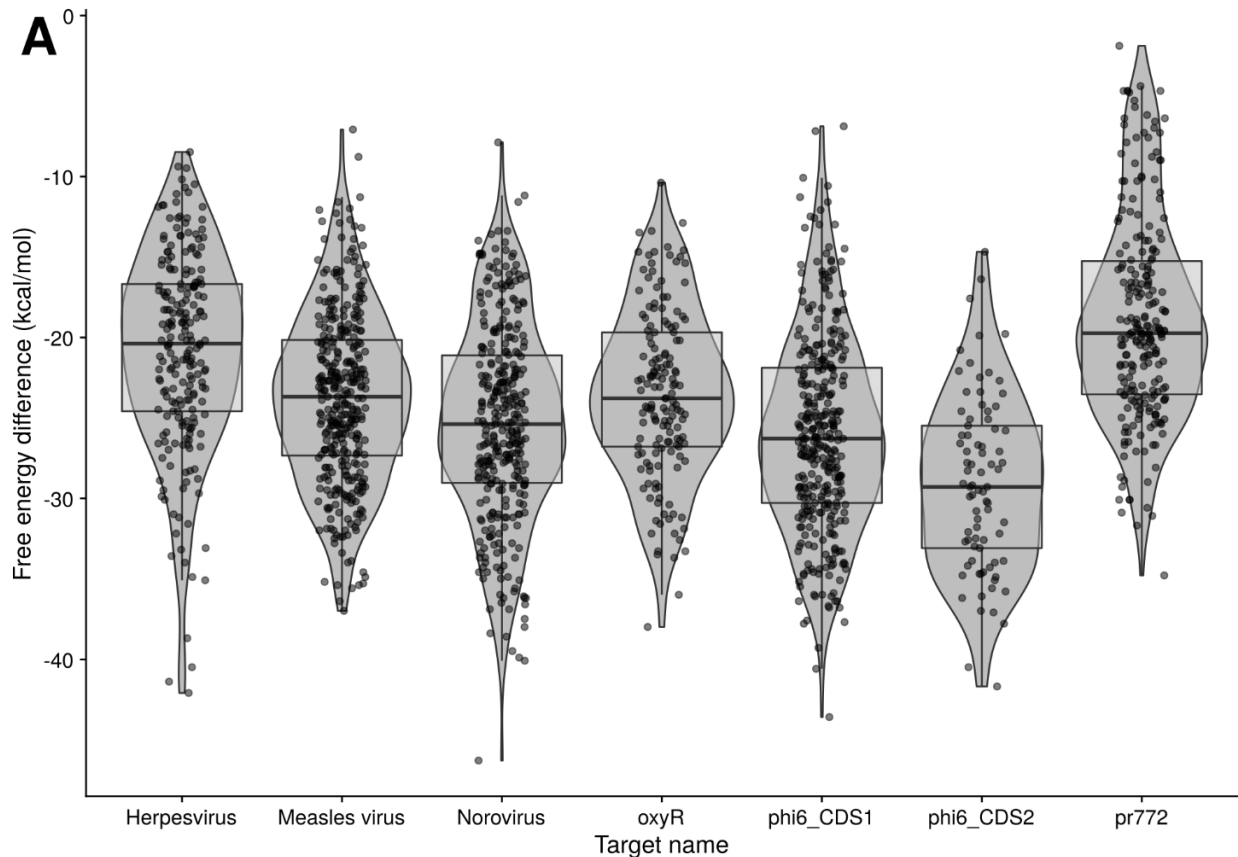
330 Similarly, using the prediction for the bound secondary structure, we can evaluate if each  
331 designed toehold riboswitch is predicted to bind to its intended target. Toehold riboswitches were  
332 classified as perfect matches if all their positions were predicted to bind to the target and imperfect  
333 matches if there was at least one mismatch. As shown in Figure 5B, around 70% of the  
334 riboswitches designed for each of our targets are predicted to bind perfectly, even when  
335 discarding all the ones that have undesirable stop codons. Thus, our riboswitches would be  
336 expected to be able to recognize their targets efficiently.  
337

338

339

340

341



343

344 **Figure 5. Analysis of binding for toehold riboswitches designed by Toeholder.** A)

345 Distribution of free energy differences between the unbound state and the bound state among the  
346 number of toehold candidates. B) Classification of toehold riboswitches according to the accuracy  
347 with which they bind to their target (imperfect and perfect match) and if they have a stop codon.

348

349

#### 350 **4.Discussion**

##### 351 *4.1 Toehold switch characterization through molecular dynamics*

352

353 Molecular dynamics simulations were first performed to get insights into the molecular interactions  
354 in the toehold structure. Our results allowed us to identify regions more likely to play an important  
355 role in the ability of switches to retain their appropriate secondary structure in the absence of the  
356 trigger. The results obtained were in line with the structural description given by Green et al.  
357 (2014). The 3D structure of the switch was stable under the conditions it was tested in (0.15M  
358 NaCl, 298.15K).

359

360 The stability of the hydrogen bonds responsible for this structure were also studied to identify  
361 weakpoints that may be worth considering when designing toehold switches. The base pairing of  
362 nucleotides at positions 23, 24, 26, 31, and 36 with their complementary sequences fluctuates  
363 the most often during the simulation, yet it is critical in preserving appropriate folding and reducing  
364 OFF signal. To reduce spurious expression of the reporting protein in absence of the target, it  
365 may be useful to favor guanine or cytosine bases in those positions to increase structural stability.  
366 Since this may also come at the cost of reduced sensitivity, additional data and *in vitro* tests are  
367 required to confirm these assumptions empirically. It is also important to remember that these  
368 weaker sites could change for toehold switches with different specifications, such as longer or  
369 shorter hairpins. Therefore, further analyses with longer simulations of more switches could help  
370 identify the positions of interest for different designs. It should also be noted that the mean  
371 occupancies presented in figure 3 were computed on a different number of hydrogen bonds  
372 depending on the type of nucleotide (A:U = 2 bonds, G:C = 3 bonds) and that it does not allow for  
373 individual characterization of those bonds. However, since only entire nucleotides can be  
374 substituted, and not individual bonds, we believe this representation remains useful to identify  
375 and consolidate structural weaknesses.

376

##### 377 *4.2 Toeholder conception*

378

379 In parallel to these experiments, we created Toeholder, an automated workflow for toehold  
380 switches design based on sequence requirements defined by Green et al. (2014). The open-  
381 source program, that can be run locally or at our web server (<https://toeholder.ibis.ulaval.ca/>),  
382 allows the users to input target sequences and receive a list of potential toehold sequences that  
383 have been curated and ranked. As a result, we believe Toeholder will contribute to a reduction of  
384 the high entry level difficulty usually associated with this molecular regulator technology.

385

386 The output of Toeholder is fully described in the Github repository. Briefly, results are organized  
387 in a folder containing copies of the input files, tables summarizing the results for all the toehold  
388 switches, and individual subfolders for each of the switches designed. Users would be  
389 encouraged to select toehold riboswitches to test experimentally based on the data available (free  
390 energy change of binding to the target, whether the toehold is predicted to bind perfectly to the  
391 trigger sequence, the desired specificity or versatility depending on matches found in genomes of  
392 interest, and the percentage of GC in weaker regions of the hairpin). Once selected, the user can  
393 find the full sequence of the riboswitch in its respective subfolder based on its index.

394  
395 Toeholder also allows users to submit genomes of interest to search for hits of the trigger  
396 sequence. This function can be used to evaluate if a riboswitch satisfies the needed requirements  
397 of target specificity or universality. For example, we tested for hits of our trigger sequences in the  
398 human genome. This allowed us to confirm that the sequences targeted by our toehold  
399 riboswitches were not present in the human genome, thus minimizing the possibility of having  
400 spurious expression due to the riboswitches interacting with human sequences. On the other  
401 hand, we looked for hits in several measles virus strains in order to make sure the trigger  
402 sequences were conserved, so that the designed riboswitches would be able to recognize many  
403 of the different strains.

404  
405 The potential improvement in sequence composition found using molecular dynamics have not  
406 been added to the program. Yet, due to its open-source nature, these modifications can be easily  
407 introduced retroactively, through the Github repository, when more robust data supports the  
408 importance of these positions in detection effectiveness. Due to temporal and monetary  
409 limitations, we were unable to experimentally assess the importance of these sites. However,  
410 since they follow experimentally validated constraints from Green et al. (2014), we believe that  
411 the toehold switches produced by Toeholder should operate in a dynamic range similar to that of  
412 the forward-engineered switches from this experimental dataset.

#### 413 414 4.3 Toeholder validation

415  
416 Toeholder was used as part of our 2019 iGEM project to design switches that could detect phages  
417 and bacterial components used for *in vitro* and proof of concept tests, as well as switches for  
418 human viruses. Additional tests were run on the outputs of the designs to validate the program.  
419 First, the secondary structure of all the riboswitches candidates for the seven targets were  
420 computed using NUPACK and all of them presented a similar structure to the one we  
421 characterized from Green et al. (2014). Therefore, we expect them to behave in a similar way *in*  
422 *vitro*. Their free energies were also recomputed and are presented in figure 5A. All switches have  
423 a negative energy that predicts they should favour the bound state to the target. In addition, of all  
424 the candidate switches produced, around 70% and up were a perfect match to the target, meaning  
425 Toeholder effectively suggested switches that would theoretically recognize their appropriate  
426 target. Altogether, the software consistently produced candidate switches that are within the  
427 defined sequence and structural restrictions and that should recognize their target, all of it in an  
428 easy-to-use format.

429



#### 430 4.4 Comparison with different approaches

431 Although the study of riboswitches is currently somewhat limited to proof-of-concept studies, *in*  
432 *silico* approaches have been widely explored for prediction of riboswitches performance both from  
433 sequence information alone (Barrick 2009; Nawrocki, Kolbe, and Eddy 2009) and structural  
434 features (Barash and Gabdank 2010). However, despite the many possibilities and applications  
435 that Toehold switches offer, far fewer studies have focused on the *in silico* design of these tools  
436 specifically ((Zadeh et al. 2011), (To et al. 2018)). The lack of high-throughput datasets on  
437 experimentally tested toeholds makes it difficult to understand what affects their performance and  
438 how it can be improved. Therefore, our open-source software, in addition to allowing the high-  
439 throughput effective design of Toehold switches, provides a global idea of their dynamics and  
440 operation. Besides its simplicity in terms of design, we have provided an *in silico* validation, which  
441 ensures an effective and working design.

442

#### 443 4.5 Limitations

444

445 The limitations of Toeholder reside in its fully *in silico* approach. Our computations may overlook  
446 sequence requirements that could only be discovered by extensive *in vitro* experiments. Very few  
447 data sets of such nature are currently available, and we were unable to complete these  
448 experiments on the switches we designed for the 2019 iGEM competition, due to time constraints.  
449 Questions also remain on the optimal physicochemical conditions to use toehold switches. Our *in*  
450 *silico* models and validation use standard conditions, in part limited by the programs, that may not  
451 reflect the way switches may want to be used. Certainly, the conditions are critical in the control  
452 of these tools since natural riboswitches can detect concentrations of small ligands (reviewed in  
453 (Findeiß et al. 2017)), but are sensitive to changes in temperature (Narberhaus 2010) or pH-value  
454 (Nechooshtan et al. 2009) which can be a limitation if conditions are no longer controlled, reducing  
455 their potential applications in very different systems or in extreme conditions. However, toehold  
456 switches address some other limitations of earlier riboregulator designs as low dynamic range,  
457 orthogonality, and programmability, since these RNA-based molecules exhibit more kinetically  
458 and thermodynamically favorable states by incorporating linear - linear interactions instead of  
459 loop-loop and loop-linear interactions (Green et al. 2014). This reflects the need for high  
460 throughput experimental screening to accompany *in silico* studies such as this one. However, our  
461 software provides a first step to facilitate high-throughput toehold switch design, production, and  
462 testing. Future studies could use it as a steppingstone to provide more in-depth characterization  
463 of these promising molecular regulators and therefore, to overcome their limitations.

464

#### 465 4.5 Applications and 2019 iGEM project

466

467 Due to their adaptability, toehold switches offer great possibilities of applications. As part of the  
468 2019 iGEM competition, we presented the project A.D.N. (Air Detector for Nucleic acids), which  
469 takes advantage of this technology to create a biosensor that detects airborne pathogens (see  
470 Team iGEM ULaval 2019 wiki: <https://2019.igem.org/Team:ULaval>). Riboswitches were designed  
471 as the sensing component of a modular device designed to sample air, extract ribonucleotides,  
472 and prepare samples via microfluidics, as well as perform detection through fluorescence

473 measurements. The combination of toehold switches with optical detection offers great practicality  
474 and target versatility.

475

476

## 477 **5.Conclusions**

478 The development of synthetic biology and the numerous molecular systems requires the parallel  
479 coupling of bioinformatics tools that facilitate their easy handling and implementation. Our open-  
480 source software, Toeholder, aims to facilitate the automated *in silico* design of toehold  
481 riboswitches and the selection of switch candidates for a target gene. Furthermore, by using  
482 molecular dynamics simulations, we identified the nucleotides in the hairpin of a reference toehold  
483 switch whose hydrogen bonds fluctuate the most. These could be potential targets to modify when  
484 polishing the design of these riboswitches. Increasing switches efficacy will likely contribute to  
485 their integration into broader applications of toehold-based technologies.

486

487

## 488 **6.Acknowledgments**

489 Special thanks to all the other members of the iGEM ULaval 2019 team (Catherine Marois, Elodie  
490 Gillard, Florian Echelard, Guillaume Fournier, Jean-Michel Proulx, Julien Roy, Karine Bouchard,  
491 Lucas Germain, Marianne Côté, Martine Voisine, Nastaran Khodaparastasarabad, Ahmed  
492 Mataich), including our professors and mentors (Hélène Deveau, Michel Guertin, Steve Charette).  
493 Team iGEM ULaval 2019 would also like to thank our partners who funded this project and  
494 covered participation fees for the competition (<https://2019.igem.org/Team:ULaval>). We would  
495 also like to thank Peng Yin and Alexander Green for kindly sharing additional raw data from their  
496 experimentally tested library of toehold switches. Funding sources had no direct involvement in  
497 study design or publication of this project.

498

## 499 **7.Data availability**

500 All data are available in the Supplementary materials.

501 DOIs:

502 Toeholder tool: <https://doi.org/10.5281/zenodo.7304556>

503 Toeholder data and Scripts: <https://doi.org/10.5281/zenodo.7304525>

504

## 505 **8.Declarations of competing interests**

506 None.

507

## 508 **9.References**

- 509 Ausländer, Simon, and Martin Fussenegger. 2014. "Toehold Gene Switches Make Big  
510 Footprints." *Nature* 516 (7531): 333–34. doi: 10.1038/516333a.
- 511 Barash, Danny, and Idan Gabdank. 2010. "Energy Minimization Methods Applied to  
512 Riboswitches: A Perspective and Challenges." *RNA Biology* 7 (1): 90–97. doi:  
513 10.4161/rna.7.1.10657.
- 514 Barrick, Jeffrey E. 2009. "Predicting Riboswitch Regulation on a Genomic Scale." *Methods in*  
515 *Molecular Biology* 540: 1–13. doi: 10.1007/978-1-59745-558-9\_1.
- 516 Blount, Kenneth F., and Ronald R. Breaker. 2006. "Riboswitches as Antibacterial Drug Targets."

- 517 *Nature Biotechnology* 24 (12): 1558–64. doi: 10.1038/nbt1268.
- 518 Camacho, Christiam, George Coulouris, Vahram Avagyan, Ning Ma, Jason Papadopoulos, Kevin  
519 Bealer, and Thomas L. Madden. 2009. “BLAST+: Architecture and Applications.” *BMC*  
520 *Bioinformatics* 10 (December): 421. doi: 10.1186/1471-2105-10-421.
- 521 Chau, Tin Hoang Trung, and Eun Yeol Lee. 2020. “Development of Cell-Free Platform-Based  
522 Toehold Switch System for Detection of IP-10 mRNA, an Indicator for Acute Kidney Allograft  
523 Rejection Diagnosis.” *Clinica Chimica Acta; International Journal of Clinical Chemistry* 510  
524 (November): 619–24. doi: 10.1016/j.cca.2020.08.034.
- 525 Chen, Vincent B., W. Bryan Arendall 3rd, Jeffrey J. Headd, Daniel A. Keedy, Robert M.  
526 Immormino, Gary J. Kapral, Laura W. Murray, Jane S. Richardson, and David C. Richardson.  
527 2010. “MolProbity: All-Atom Structure Validation for Macromolecular Crystallography.” *Acta*  
528 *Crystallographica. Section D, Biological Crystallography* 66 (Pt 1): 12–21. doi:  
529 10.1107/S0907444909042073.
- 530 Dirks, Robert M., and Niles A. Pierce. 2003. “A Partition Function Algorithm for Nucleic Acid  
531 Secondary Structure Including Pseudoknots.” *Journal of Computational Chemistry* 24 (13):  
532 1664–77. doi: 10.1002/jcc.10296.
- 533 Findeiß, Sven, Maja Etzel, Sebastian Will, Mario Mörl, and Peter F. Stadler. 2017. “Design of  
534 Artificial Riboswitches as Biosensors.” *Sensors* 17 (9). doi:10.3390/s17091990.
- 535 Garst, Andrew D., Andrea L. Edwards, and Robert T. Batey. 2011. “Riboswitches: Structures and  
536 Mechanisms.” *Cold Spring Harbor Perspectives in Biology* 3 (6). doi:  
537 10.1101/cshperspect.a003533.
- 538 Green, Alexander A., Jongmin Kim, Duo Ma, Pamela A. Silver, James J. Collins, and Peng Yin.  
539 2017. “Complex Cellular Logic Computation Using Ribocomputing Devices.” *Nature* 548  
540 (7665): 117–21. doi: 10.1038/nature23271.
- 541 Green, Alexander A., Pamela A. Silver, James J. Collins, and Peng Yin. 2014. “Toehold Switches:  
542 De-Novo-Designed Regulators of Gene Expression.” *Cell* 159 (4): 925–39. doi:  
543 10.1016/j.cell.2014.10.002.
- 544 Gupta, Angela, and D. Swati. 2019. “Riboswitches in Archaea.” *Combinatorial Chemistry & High*  
545 *Throughput Screening* 22 (2): 135–49. doi: 10.2174/1386207322666190425143301.
- 546 Humphrey, W., A. Dalke, and K. Schulten. 1996. “VMD: Visual Molecular Dynamics.” *Journal of*  
547 *Molecular Graphics* 14 (1): 33–38, 27–28. doi: 10.1016/0263-7855(96)00018-5.
- 548 Jo, Sunhwan, Taehoon Kim, Vidyashankara G. Iyer, and Wonpil Im. 2008. “CHARMM-GUI: A  
549 Web-Based Graphical User Interface for CHARMM.” *Journal of Computational Chemistry* 29  
550 (11): 1859–65. doi: 10.1002/jcc.20945.
- 551 Lee, Jumin, Xi Cheng, Jason M. Swails, Min Sun Yeom, Peter K. Eastman, Justin A. Lemkul,  
552 Shuai Wei, et al. 2016. “CHARMM-GUI Input Generator for NAMD, GROMACS, AMBER,  
553 OpenMM, and CHARMM/OpenMM Simulations Using the CHARMM36 Additive Force Field.”  
554 *Journal of Chemical Theory and Computation* 12 (1): 405–13. doi: 10.1021/acs.jctc.5b00935.
- 555 Ma, Duo, Luhui Shen, Kaiyue Wu, Chris W. Diehnelt, and Alexander A. Green. 2018. “Low-Cost  
556 Detection of Norovirus Using Paper-Based Cell-Free Systems and Synbody-Based Viral  
557 Enrichment.” *Synthetic Biology* 3 (1): ysy018. doi: 10.1093/synbio/ysy018.
- 558 Magro, Laura, Béatrice Jacquelin, Camille Escadafal, Pierre Garneret, Aurélia Kwasiborski, Jean-  
559 Claude Manuguerra, Fabrice Monti, et al. 2017. “Paper-Based RNA Detection and  
560 Multiplexed Analysis for Ebola Virus Diagnostics.” *Scientific Reports* 7 (1): 1347. doi:  
561 10.1038/s41598-017-00758-9.
- 562 Mandal, Maumita, and Ronald R. Breaker. 2004. “Adenine Riboswitches and Gene Activation by  
563 Disruption of a Transcription Terminator.” *Nature Structural & Molecular Biology* 11 (1): 29–  
564 35. doi: 10.1038/nsmb710.
- 565 Narberhaus, Franz. 2010. “Translational Control of Bacterial Heat Shock and Virulence Genes by  
566 Temperature-Sensing mRNAs.” *RNA Biology* 7 (1): 84–89. doi: 10.4161/rna.7.1.10501.
- 567 Nawrocki, E. P., D. L. Kolbe, and S. R. Eddy. 2009. “Infernal 1.0: Inference of RNA Alignments.”

- 568 *Bioinformatics*. <https://doi.org/10.1093/bioinformatics/btp326>. doi:  
569 10.1093/bioinformatics/btp157.
- 570 Nechooshtan, Gal, Maya Elgrably-Weiss, Abigail Sheaffer, Eric Westhof, and Shoshy Altuvia.  
571 2009. "A pH-Responsive Riboregulator." *Genes & Development* 23 (22): 2650–62. doi:  
572 10.1101/gad.552209.
- 573 Nshogozabahizi, J. C., K. L. Aubrey, J. A. Ross, and N. Thakor. 2019. "Applications and  
574 Limitations of Regulatory RNA Elements in Synthetic Biology and Biotechnology." *Journal of*  
575 *Applied Microbiology* 127 (4): 968–84. doi: 10.1111/jam.14270.
- 576 Park, Soan, and Jeong Wook Lee. 2021. "Detection of Coronaviruses Using RNA Toehold Switch  
577 Sensors." *International Journal of Molecular Sciences* 22 (4).  
578 <https://doi.org/10.3390/ijms22041772>. doi: 10.3390/ijms22041772.
- 579 Phillips, James C., Rosemary Braun, Wei Wang, James Gumbart, Emad Tajkhorshid, Elizabeth  
580 Villa, Christophe Chipot, Robert D. Skeel, Laxmikant Kalé, and Klaus Schulten. 2005.  
581 "Scalable Molecular Dynamics with NAMD." *Journal of Computational Chemistry*, Springer  
582 Seri, 26 (16): 1781–1802. doi: 10.1002/jcc.20289.
- 583 Popenda, Mariusz, Marta Szachniuk, Maciej Antczak, Katarzyna J. Purzycka, Piotr Lukasiak,  
584 Natalia Bartol, Jacek Blazewicz, and Ryszard W. Adamiak. 2012. "Automated 3D Structure  
585 Composition for Large RNAs." *Nucleic Acids Research* 40 (14): e112. doi:  
586 10.1093/nar/gks339.
- 587 Purzycka, K. J., M. Popenda, M. Szachniuk, M. Antczak, P. Lukasiak, J. Blazewicz, and R. W.  
588 Adamiak. 2015. "Automated 3D RNA Structure Prediction Using the RNAComposer Method  
589 for Riboswitches1." In *Methods in Enzymology*, edited by Shi-Jie Chen and Donald H. Burke-  
590 Aguero, 553:3–34. Academic Press. . doi: 10.1016/bs.mie.2014.10.050.
- 591 Serra, Martin J., and Douglas H. Turner. 1995. "Predicting Thermodynamic Properties of RNA."  
592 In *Methods in Enzymology*, 259:242–61. Academic Press. doi: 10.1016/0076-  
593 6879(95)59047-1.
- 594 Sudarsan, Narasimhan, Jeffrey E. Barrick, and Ronald R. Breaker. 2003. "Metabolite-Binding  
595 RNA Domains Are Present in the Genes of Eukaryotes." *RNA* 9 (6): 644–47. doi:  
596 10.1261/rna.5090103.
- 597 To, Andrew Ching-Yuet, David Ho-Ting Chu, Angela Ruoning Wang, Frances Cheuk-Yau Li, Alan  
598 Wai-On Chiu, Daisy Yuwei Gao, Chung Hang Jonathan Choi, et al. 2018. "A Comprehensive  
599 Web Tool for Toehold Switch Design." *Bioinformatics* 34 (16): 2862–64. doi:  
600 10.1093/bioinformatics/bty216.
- 601 Winkler, Wade, Ali Nahvi, and Ronald R. Breaker. 2002. "Thiamine Derivatives Bind Messenger  
602 RNAs Directly to Regulate Bacterial Gene Expression." *Nature* 419 (6910): 952–56. doi:  
603 10.1038/nature01145.
- 604 Zadeh, Joseph N., Conrad D. Steenberg, Justin S. Bois, Brian R. Wolfe, Marshall B. Pierce, Asif  
605 R. Khan, Robert M. Dirks, and Niles A. Pierce. 2011. "NUPACK: Analysis and Design of  
606 Nucleic Acid Systems." *Journal of Computational Chemistry* 32 (1): 170–73. doi:  
607 10.1002/jcc.21596.
- 608 Zuker, Michael. 2003. "Mfold Web Server for Nucleic Acid Folding and Hybridization Prediction."  
609 *Nucleic Acids Research* 31 (13): 3406–15. doi: 10.1093/nar/gkg595.

## 610 **10. Supplementary data**

611 Supplementary video 1: <https://doi.org/10.5281/zenodo.7418392>

612